An extended equal-area criterion for transient stability assessment in GFM integrated power systems

Yujin Lee[1], Byungchan Yoo[1], Jaesung Hwang[1], Yeuntae Yoo[2], Seungmin Jung[1]*
[1]Department of Electrical and Computer Engineering, University of Seoul, Seoul, Republic of Korea
[2]Department of Electrical Engineering, Myongji University, Yongin, Republic of Korea
dldbtrue@uos.ac.kr, ybc5075@uos.ac.kr, jaesungh@uos.ac.kr, ytyoo@mju.ac.kr, seungminj@uos.ac.kr

Abstract— **The increasing penetration of renewable energy resources has significantly reduced system inertia, thereby weakening the transient stability of modern power grids. This paper presents an extended Equal-Area Criterion (EAC) framework for quantitatively evaluating the dynamic contribution of grid-forming (GFM) inverters in hybrid synchronous generator (SG)–GFM systems. The proposed method incorporates the critical clearing time (CCT) into the EAC formulation, enabling assessment of the transient stability margin under severe disturbances. Using the developed analytical model, the minimum GFM capacity required to maintain stability equivalent to that of conventional SG-based systems is systematically determined. Simulation results on a benchmark test system validate the effectiveness of the proposed approach and demonstrate that GFM control substantially enhances transient stability in converter-dominated, renewable-integrated power systems.**

Index Terms—**critical clearing time, equal-area criterion, grid-forming inverter, transient stability.**

I. Introduction

The rapid global transition toward renewable energy has accelerated the integration of inverter-based resources (IBRs), such as photovoltaic (PV) and wind power systems, into modern power grids. As the proportion of IBRs continues to increase, the conventional synchronous generator (SG)-dominated structure is being replaced by converter-interfaced units, resulting in a significant reduction in system inertia and damping capability [1]. This reduction has been recognized as a major factor that weakens frequency and transient stability under large disturbances. Consequently, maintaining stability in low-inertia networks has become a critical issue in next-generation power system operation.

This issue is strongly associated with the grid-following (GFL) control strategy, which is widely adopted in renewable-based generation systems. Since the GFL scheme depends on an external grid reference through phase-locked loop (PLL) - based synchronization, its ability to actively regulate voltage and frequency during disturbances is limited, especially under weak-grid conditions [2].

Recent research has analyzed the stability characteristics of GFL inverters under weak-grid environments [3], [4]. For instance, [3] presented an Equal-Area Criterion (EAC)-based approach incorporating PLL dynamics to assess transient margins, while [4] extended the analysis to identify stable operating regions using detailed inverter models. Although these studies have contributed to understanding the dynamic behavior of GFL inverters, their applicability is often restricted to single-inverter scenarios and steady-state operating points, providing limited insight into large-scale transient phenomena.

To overcome these limitations, grid-forming (GFM) inverter control has emerged as a viable alternative for stabilizing converter-dominated systems. Unlike GFL inverters, GFM inverters autonomously establish voltage and frequency references, thereby contributing synthetic inertia and improving dynamic performance. Control strategies such as droop-based control and virtual synchronous machine (VSM) control have been developed to emulate the electromechanical response of SGs and enhance transient resilience during grid faults [5].

However, most existing studies on GFM inverters have concentrated on small-signal stability analysis [6], [7]. Although such analysis provides valuable insights around nominal operating conditions, it cannot accurately represent nonlinear system behavior during large disturbances such as transmission-line faults or generator outages. Moreover, there is still no systematic methodology to determine the minimum GFM capacity required to preserve transient stability equivalent to that of SG–dominated systems.

To address these issues, this paper proposes an extended EAC framework applicable to hybrid systems comprising both SGs and GFM inverters. The proposed method incorporates the dynamic characteristics and power–angle relationship of GFM units, enabling quantitative evaluation of their contribution to system transient stability. Using this enhanced criterion, the minimum GFM penetration level required to maintain

This work was partly supported by Korea Institute of Energy Technology Evaluation and Planning (KETEP) grant funded by the Korea government (MOTIE) (RS-2023-00234563, Development of power system modeling & analysis and interoperability evaluation technology applied with grid forming based on distributed energy) and Korea Electric Power Corporation grant funded by the Korean government (R25XO03-8).

979-8-3315-8138-1

equivalent transient performance can be determined. The proposed framework is validated through simulations on an IEEE standard test system, confirming its effectiveness and practical applicability for stability assessment in future converter-dominated grids.

II. THEORETICAL BACKGROUND

A. SG-GFM test system

The test system considered in this study consists of a conventional SG and GFM inverters interconnected through a common transmission network. The configuration represents a simplified model of a low-inertia power system in which the conventional SG capacity is partially replaced by GFM units. Each GFM inverter autonomously establishes voltage and frequency references through an internal control loop, while the SG maintains its conventional swing dynamics. The hybrid system is modeled to analyze the electromechanical interaction between the SG rotor and the GFM virtual angle during post-fault conditions.

B. Transient Stability Analysis Based on the EAC

Compared with conventional SG-based systems, inverter-based renewable resources exhibit distinct dynamic behaviors that directly affect system reliability and security. Among the key aspects of dynamic stability—namely, transient, small-signal, and frequency stability—transient stability is of primary importance when evaluating the system response to severe disturbances such as short circuits or sudden load changes [8], [9]. Transient stability determines whether generators can maintain synchronism and reach a new steady-state equilibrium by balancing the mechanical input and electrical output powers following a disturbance [10].

The electromechanical dynamics of a SG during a disturbance are governed by the classical swing equation, expressed as

$$M\frac{d^2\delta}{dt^2} + D\frac{d\delta}{dt} = P_m - P_e \quad (1)$$

Where M is the inertia constant, D represents the damping coefficient, P_m is the mechanical input power, P_e is the electrical output power, and δ is the rotor angle.

The EAC provides an analytical method to assess transient stability by applying the principle of energy balance between the accelerating and decelerating phases of the generator. The instantaneous accelerating power can be defined as

$$P_a = P_m - P_e \quad (2)$$

and the electrical power output is expressed as

$$P_e = \frac{E' V_{bus}}{X_{eq}} sin\delta \quad (3)$$

E' denotes the internal voltage of the generator, and X_{eq} represents the equivalent reactance between the generator and the infinite bus. Based on the relationship between P_m and P_e, the acceleration energy (A_{acc}) and deceleration energy (A_{dec}) are defined as follows.

$$A_{acc} = \int_{\delta_0}^{\delta_c} (P_m - P_e)\, d\delta \quad (4)$$

$$A_{dec} = \int_{\delta_c}^{\delta_{max}} (P_e - P_m)\, d\delta \quad (5)$$

Where δ_0 is the pre-fault rotor angle, δ_c is the fault clearing angle, and δ_{max} denotes the maximum swing angle reached after the disturbance.

During a disturbance, the generator accelerates when the P_m exceeds the P_e, resulting in increased rotor speed and the accumulation of kinetic energy. Conversely, when P_m is less than P_e, the generator decelerates and releases stored energy. The generator maintains synchronism when the total accelerating and decelerating energies are equal, i.e.,

$$A_{acc} = A_{dec} \quad (6)$$

This equality defines the critical clearing condition beyond which the system loses stability. If the A_{acc} is completely compensated by the A_{dec} (i.e., $A_{acc} = A_{dec}$), the rotor settles to a new equilibrium, and synchronism is preserved. However, when $A_{acc} > A_{dec}$, the generator cannot restore synchronism, resulting in a loss of stability and system separation.

C. GFM Inverter

GFM inverters operate with a control strategy that allows them to establish voltage and frequency independently within the grid, thereby functioning as voltage sources under ideal operating conditions [5]. Droop-based control, considered the most basic method among GFM inverter strategies, regulates frequency and voltage by mathematically emulating the power–frequency and voltage–reactive power characteristics of a SG. The basic principle of droop control can be expressed as follows:

$$\omega = \omega_0 - k_p(P - P_0) \quad (7)$$

$$V = V_0 - k_q(Q - Q_0) \quad (8)$$

Where ω and V denote the output frequency and voltage magnitude of the inverter, respectively, while P and Q represent the measured active and reactive powers. K_p and K_q are the droop coefficients that determine the rate of change of frequency and voltage, and ω_0 and V_0 are the nominal reference frequency and voltage under steady-state conditions.

The VSM control extends the droop-based control by incorporating virtual inertia and damping characteristics to reproduce the swing equation of SG.

$$M_{vir}\frac{d^2\delta}{dt^2} + D_{vir}\frac{d\delta}{dt} = P_m - P_e \quad (9)$$

Where M_{vir} and D_{vir} denote the virtual inertia and damping coefficients, respectively. Through this mechanism, the inverter can mitigate the frequency nadir and enhance transient stability during disturbances. The combination of these two control methods enables the system to exhibit transient responses equivalent to those of an SG-based power system.

III. GFM Application based on EAC

A. Estimation of required GFM capacity

To reflect voltage depression during faults without assuming an infinite-bus grid, the electrical power–angle characteristics used in the EAC are evaluated from stage-dependent network equivalents at the PCC. Specifically, a Thevenin equivalent is obtained for the pre-fault, fault-on, and post-fault stages, yielding $P{-}\delta$ curves that capture the change in transfer capability due to network topology and voltage variations.

$$P_{tie} = \frac{EV}{X_{tie}}\sin(\delta_{SG} - \delta_{GFM}) \tag{10}$$

Where X_{tie} is the equivalent reactance of the tie-line. During severe faults, the GFM converter output is constrained by the inner current controller and the current limiting logic. Let $I_{\max}$ denote the converter current limit and i_q the commanded reactive current. The available active current is bounded by

$$i_d^{max} = \sqrt{I_{max}^2 - i_q^2}, \tag{11}$$

which yields an instantaneous active-power ceiling

$$P_{max}(t) = \frac{3}{2}V_{PCC}(t)i_d^{max}. \tag{12}$$

Accordingly, the transferable tie-line power in (10) is modified to a current-limited form

$$P_{tie}^{\lim}(\delta, t) = \mathrm{sign}(\sin\delta)\min\left(\left|\frac{EV_{PCC}(t)}{X_{tie}}\sin\delta\right|, P_{max}(t)\right), \tag{13}$$

and the EAC integrals are evaluated using $P_{tie}^{\lim}$, resulting in conservative stability margins under fault-induced voltage dips.

The relative angle $\delta = \delta_{SG} - \delta_{GFM}$ governs the active power exchange and thus determines transient stability. By considering damping coefficient of sources (D_{SG}, D_{GFM}) yields the combined swing dynamics:

$$M_{eq}\frac{d^2\delta}{dt^2} + D_{eq}\frac{d\delta}{dt} = P_{m,SG} - P_{ref,GFM} - P_{tie} \tag{14}$$

For the angle coordinate $\delta = \delta_{SG} - \delta_{GFM}$, the equivalent inertia associated with the relative motion is obtained from kinetic-energy equivalence, leading to the reduced inertia

$$M_{eq} = \frac{M_{SG}M_{GFM}}{M_{SG}+M_{GFM}} \tag{15}$$

while D_{eq} is defined consistently for the relative mode and is validated against EMT simulations.

Equation (14) describes the coupled electromechanical dynamics between the SG and GFM inverter and forms the basis for the transient stability analysis. The corresponding output control is implemented in a detailed PSCAD model, and an equivalent scaling model is additionally employed to integrate the detailed GFM output into the transmission system. The configuration enables the expanded GFM output to be supplied at the connection point, as illustrated in Fig. 1.

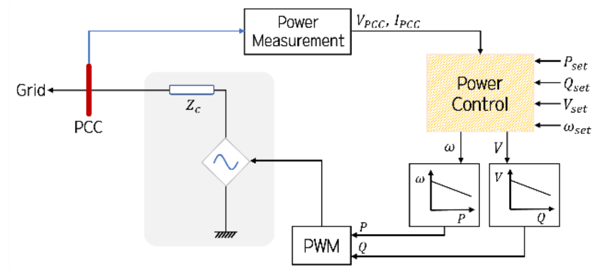

Figure 1. Applied lumped GFM model for PSCAD

This study considers the transient stability of the SG–GFM combined system and determines the minimum GFM penetration level (α_{GFM}) required to maintain an equivalent stability margin to that of a conventional SG-only system. The stability margin is defined by the critical clearing angle derived from the extended EAC. The problem can be formulated with finding α_{GFM} with

$$EAC(\alpha_{GFM^*}) = EAC_{SG} \tag{16}$$

Subject to: $0 < \alpha_{GFM} < 1$,

$$P_{m,SG} = P_{e,SG} + P_{tie},\ P_{ref,GFM} = P_{e,GFM} + P_{tie} \tag{17}$$

The derived model in (10) – (17) provides a unified analytical basis for quantifying the transient behavior of the combined system.

B. Critical Clearing Angle and Transient Stability Margin

The critical clearing angle (δ_{cl}) is defined as the maximum rotor angle that can tolerate without losing synchronism following fault clearance. This value represents the boundary between stable and unstable operating conditions, as illustrated in Fig. 2. When the fault is cleared before than δ_{cl}, energy balance is preserved and the generator returns to synchronism. Conversely, if fault clearing occurs after δ_{cl}, the accelerating energy exceeds the decelerating energy, leading to an irreversible increase in rotor speed and eventual instability [11].

In the time domain, the δ_{cl} corresponds to a specific instant known as the critical clearing time (CCT). The CCT is defined as the maximum permissible fault duration before loss of synchronism occurs [12]. It can be expressed as the time required for the rotor to reach δ_{cl} during the accelerating phase:

$$t_{CCT} = \int_{\delta_0}^{\delta_{cl}} \frac{d\delta}{\omega} \tag{18}$$

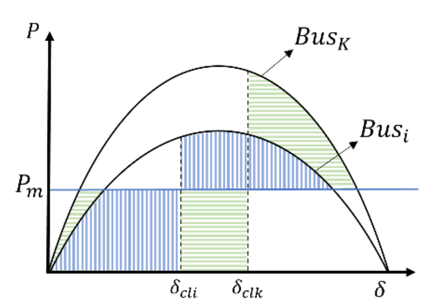

Figure 2. Transient stability margin

979-8-3315-8138-1

Where δ_0 is the pre-fault rotor angle and ω denotes the instantaneous angular velocity of the generator. If the fault persists longer than t_{CCT}, the generator angle will exceed δ_{cl}, causing loss of synchronism. Thus, t_{CCT} serves as a practical indicator of the system's transient stability margin.

The proposed method for evaluating the transient stability margin is illustrated in Fig. 3. This approach utilizes CCT to determine the required GFM capacity. First, calculate the base-case CCT of the SG–only system. Subsequently, a phase-out bus is selected, and its SG is replaced with a GFM inverter. The resulting change in CCT from the GFM replacement is computed, and the stability of the hybrid system is assessed. If the stability criterion is not satisfied, the GFM capacity is adjusted, and the process is repeated. This iterative procedure determines the required necessary to achieve stability equivalent to that of the reference system. The proposed extended EAC is intended to capture the electromechanical time-scale stability margin (angle/frequency dynamics) and to provide a planning-oriented sizing/allocation guideline. Sub-cycle phenomena and converter inner-loop instabilities are not explicitly modeled in the analytical derivation; therefore, all key conclusions are cross-validated using EMT simulations that include the detailed inner current control and current limiting.

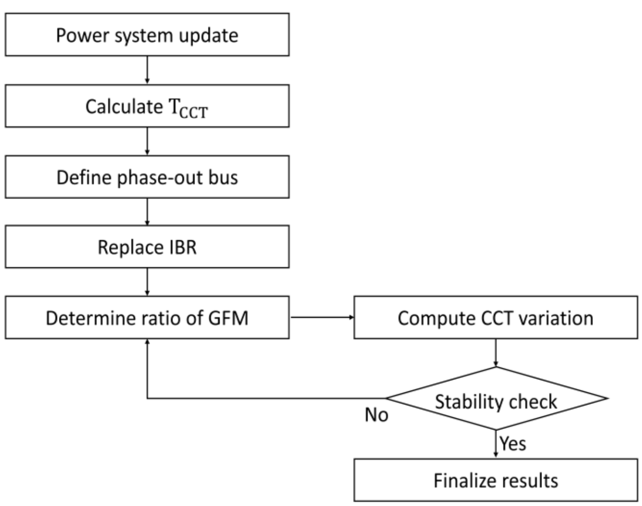

Figure 3. Flowchart to determine the required α_{GFM} based on CCT

TABLE I. MODIFICTION FOR GFM ASSIGNMENT – IEEE 39

Bus number	Calculated CCT	Assigned GFM	
		Case1	Case2
33	0.3425	166.6	167
34	0.3444	166.6	130
36	0.3394	166.6	203

TABLE II. MODIFIED LOADS – IEEE 39

Bus number	Reactive power	Active power
16	50 Mvar	150 MW
20	50 Mvar	250 MW
21	70 Mvar	120 MW
23	80 Mvar	130 MW

IV. SIMULATION

A. *Simulation configuration*

To validate the effectiveness of the proposed transient stability assessment method, electromagnetic transient simulations were performed on the IEEE 39-bus test system. The δ_{cl} of each SG was first obtained using the extended EAC, and the corresponding CCT was derived to quantify the transient stability margin.

Three SGs located near the contingency location were selected for replacement, and the following scenarios were designed:

- Case 1 – Mixed GFL/GFM replacement: a total of 500 MW of IBRs is integrated, where the GFM capacity is uniformly distributed across the three buses.
- Case 2 – Proposed CCT-based GFM allocation: The same total GFM capacity (500 MW) is deployed, but the allocation ratio at each replacement bus is determined according to the CCT-based penetration criterion developed in this study.

Table I summarizes the ratings of the SG units selected for replacement. For Case 1 and Case 2, the aggregate GFM capacity is fixed at 500 MW, and only the distribution among buses differs depending on the applied method. To evaluate the impact of introducing grid-forming control, the load buses in the original system were modified as shown in Table II.

B. *Results*

The simulations were performed in PSCAD/EMTDC. A three-phase fault scenario was applied at the transmission line between Bus 24 and Bus 25, and the line was tripped after five cycles. Fig. 4 presents the simulation results for this scenario. While all results were confirmed to have stabilized, the figures are shown on an enlarged scale to clearly illustrate detailed dynamic characteristics.

In Case 1 (uniform 500 MW GFM), the trajectories remain bounded but exhibit a larger steady-state angle separation than the SG baseline case, and the frequency nadir is reduced to 54.61 Hz. This indicates insufficiently targeted stabilizing support.

In Case 2 (proposed CCT-based allocation with the same 500 MW total), the post-disturbance trajectories most closely track the SG baseline compared to Case1, and the angle spread is reduced. Additionally, the frequency nadir reaches 58.96 Hz, showing the closest performance to the SG baseline case.

TABLE III. NUMERICAL RESULTS IN THE SCENARIOS

	Base case	Case 1	Case 2
Total supply [MW]	6616.9	6619	6619.4
Total load [MW]	6585.51	6585.77	6585.87
Frequency nadir [Hz]	59.58	54.61	58.96
Angle spread	51.6	113.19	73.82
Angle stability	Stable	Stable	Stable

979-8-3315-8138-1

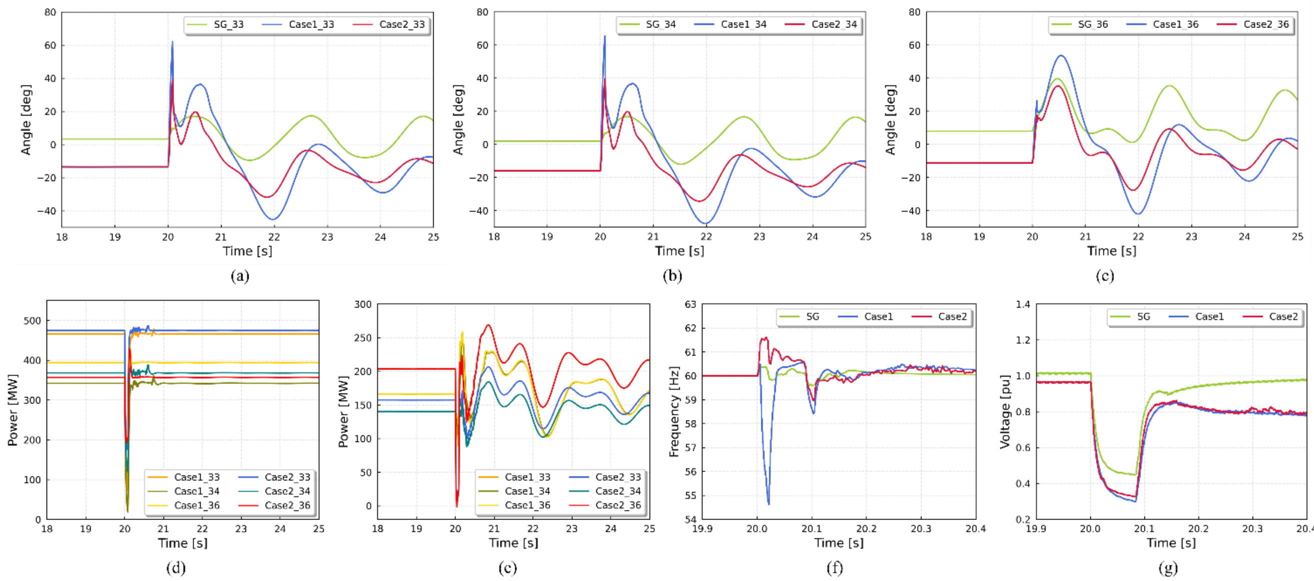

Figure 4. Result of simulation: (a) angle state at bus 33; (b) angle state at bus 34; (c) angle state at bus 36; (d) active power output of GFL at selected bus; (e) active power output of GFM at selected bus; (f) frequencies; (g) voltages

Although 500 MW of GFM capacity uniformly distributed across the three buses, the post-fault angle trajectories remain bounded, demonstrating the stabilizing contribution of GFM control. However, the steady-state response still deviates from the nominal SG-based result. This deviation indicates that the uniform allocation fails to sufficiently concentrate inertial and damping support at the most sensitive locations, thereby limiting the improvement in transient stability. By contrast, when the same total GFM capacity is allocated according to the CCT-derived ratio, the transient response improves further. These results confirm that allocating the same GFM budget according to the CCT-derived sensitivity yields more effective transient stabilization than uniform deployment. A summary of the overall simulation results is provided in Table III.

V. Conclusion

This paper presented an extended transient stability assessment framework for renewable-integrated, low-inertia power systems. By incorporating GFM dynamics into the classical EAC, the proposed method enables a quantitative evaluation of the stabilizing contribution of GFM inverters. The CCT was utilized to determine the minimum GFM capacity required to achieve a stability margin equivalent to that of conventional SG–based systems. Simulation studies on the IEEE 39-bus test system demonstrated that allocating GFM capacity based on the proposed CCT-derived guideline substantially improves transient stability under severe disturbances. In particular, the CCT-based allocation approach yielded post-fault angle trajectories closely matching those of the original SG system, outperforming both GFL-only and uniformly distributed GFM configurations. The results confirm that GFM inverters provide essential synthetic inertia and damping support in converter-dominated grids, and their strategic deployment is critical for maintaining synchronism in future low-inertia power systems with high renewable penetration.

References

[1] P. Tielens, D. V. Hertem, “The relevance of inertia in power systems,” Renewable and Sustainable Energy Reviews, vol. 55, pp. 999-1009, 2016.

[2] Yitong Li, Yunjie Gu & Timothy C. Green, “Revisiting Grid-Forming and Grid-Following Inverters: A Duality Theory”, IEEE Transactions on Power Systems, Vol 37, No 6, November 2022

[3] Q. Hu, L. Fu, F.Ma, and F. Ji, “Large signal synchronizing instability of PLL-based VSC connected to weak AC grid,” IEEE Trans. Power Syst., vol. 34, no. 4, pp. 3220–3229, Jul. 2019.

[4] W. Wang, G. M. Huang, D. Ramasubramanian, and E. Farantatos, “Transient stability analysis and stability margin evaluation of phaselocked loop synchronised converter-based generators,’’ IET Gener., Transmiss. Distrib., vol. 14, no. 22, pp. 5000–5010, Nov. 2020.

[5] Rathnayake, Dayan B., et al. "Grid forming inverter modeling, control, and applications." Ieee Access, vol. 9, pp. 114781-114807, 2021.

[6] H. Wu et al., “Small-signal modeling and parameters design for virtual synchronous generators,” IEEE Trans. Ind. Electron., vol. 63, no. 7, pp. 4292–4303, Jul. 2016.

[7] Singh, Arshpreet, et al. "Slow-interaction converter-driven stability in the distribution grid: Small-signal stability analysis with grid-following and grid-forming inverters." IEEE Transactions on Power Systems 39.2, 4521-4536, 2023.

[8] Hatziargyriou, Nikos, et al. "Definition and classification of power system stability–revisited & extended." IEEE Transactions on Power Systems 36.4, 3271-3281, 2020.

[9] L. Shi, S. Sun, L. Yao, Y. Ni, and M. Bazargan, “Effects of wind generation intermittency and volatility on power system transient stability,” IET Renewable Power Generation, vol. 8, no. 5, pp. 509-521, 2014.

[10] Machowski, Jan, et al. Power system dynamics: stability and control. John Wiley & Sons, 2020.

[11] P. W. Sauer and M. A. Pai, Power System Dynamics and Stability. Upper Saddle River, N.J.: Prentice Hall, 2017.

[12] O. Lenga, “Application of critical clearing time as a transient stability criterion for power system expansion planning,” 2014 IEEE International Conference on Intelligent Energy and Power Systems (IEPS), pp. 215-218, 2014.

979-8-3315-8138-1